



Accurate Estimating of Mechanical Properties of Austenitic Stainless Steels with Residual Stresses Using Indentation Technique

F. Barati, R. Moharrami*

Department of Mechanical Engineering, University of Zanjan, Zanjan, Iran

ABSTRACT: This study considers the accurate determination of the mechanical properties of austenitic steels containing equibiaxial residual stress by the spherical indentation technique. Many numerical simulations have been developed to evaluate the accuracy of the Kim and Lee methods. The results revealed that the Kim method evaluates a specimen's mechanical properties with higher accuracy than the Lee method. The Kim method was utilized in this paper to investigate the effect of residual stress on the accuracy of the indentation technique. The results of the study showed that residual stresses could lead to significant errors in the results of estimating the properties of materials like elasticity module, yield strength, and work hardening. By formulating the error changes as a function of work hardening and normalized residual stress, a method has been proposed to reduce the error. The proposed method has significantly mitigated the error in estimating the properties of materials with residual stress through the Kim method. Based on the results, the absolute value of errors has decreased from a maximum of 48% for E , 33% for σ_y , and 39% for n to 12%, 1%, and 3% respectively. Experimental tests on the stainless steel 321 sample were used to validate the results, and by comparing the numerical results, it was shown that a more accurate value for the properties of materials could be obtained using the proposed method.

Review History:

Received: Nov. 27, 2021
Revised: May, 23, 2022
Accepted: Jun. 08, 2022
Available Online: Jul. 01, 2022

Keywords:

Mechanical properties
Instrumented indentation test
Residual stresses
Austenitic stainless steel

1- Introduction

The effects of residual stress on materials are important. To consider these effects in engineering design, the properties of stressed materials should be measured. Indentation is a portable non-destructive method that has been used in recent years for this purpose. Using this method in addition to residual stresses, the mechanical properties of a specimen can be estimated. Some researchers have used this method in their studies due to its special features.

Tabor [1] determined properties by experimental tests. Although these properties are classified as intrinsic characteristics of materials, Doerner and Nix [2] demonstrated that the mechanical behavior of the materials could be affected by various factors, such as stress, temperature, radiation, and time. To assess the health of the engineered structures and their future performance, it is essential to periodically evaluate the mechanical behavior of structures considering the loading process. The tests for determining the mechanical properties of materials are divided into destructive and non-destructive tests. The destructive tests (e.g., tensile tests) provide more reliable results than the non-destructive tests. However, these tests cannot be used for the under-operation parts. Thus, researchers have attempted to develop non-destructive tests to evaluate the mechanical behavior of the established parts. In recent years, various

techniques have been developed for the non-destructive evaluation of mechanical behavior. The indentation is one of the techniques, and it is a portable approach. In this technique, the material behavior is examined via an indenter during the loading and unloading processes. Thus, some properties of the materials are estimated, encompassing elastic modulus, yield stress, and work hardening coefficient. This technique has comparative advantages over the other techniques. Different research has been developed to characterize the applications of this technique, identify the causes of errors, and improve its accuracy. Since the residual stresses have a significant impact on the indentation phenomenon, they are taken into account as the most vital factors affecting the estimation of mechanical properties in the Instrumented Indentation Test (IIT).

Lee et al. [3] developed a study to determine the homogenous elastic-plastic properties of materials using a circular indenter and applying numerical and experimental methods. They implemented several interpolation steps and formulated the material properties as a function of the work hardening coefficient and yield strain. This procedure has been performed by deriving the fixed regression coefficients. Kim et al. [4] utilized the indentation technique to estimate the tensile properties of materials and draw the stress-strain curve. This process has been carried out by using a circular indenter. The results demonstrated that the accuracy of this method depended considerably on the way of analyzing

*Corresponding author's email: r_moharrami@znu.ac.ir



contact depth and definitions of stress and strain.

Lee et al. [5] studied spherical indentation based on numerical analysis and experiment to develop robust testing techniques to evaluate metal's isotropic elastic-plastic properties. The representative stress and plastic strain concept are critically investigated via finite element analysis, and some conditions for the representative values are suggested. Boschetto et al. [6] employed the indentation technique to determine the mechanical properties of steel parts. They cut steel discs of C40 from an extruded bar and then machined them by facing operation under various conditions. Also, they utilized indenters with diameters of 1 and 2 mm made of tungsten carbide to calculate the yield strength and indentation pressure corresponding to each diameter.

Chunyu et al. [7] have found noticeable degradation of the measured elastic moduli of ductile metals in meso/macro indentation tests. Finite element simulations show that the finite stiffness of an indentation system can cause a false degradation of the effective indentation modulus.

Chang et al. [8] analytically described a new insight into the relationship between constraint factors of stress and strain based on the formation of Tabor's equation. Spherical indentation tests were performed to evaluate these constraint factors.

Zhang et al. [9] proposed an analytical method based on the extended expanding cavity model to determine the proof strength $R_{p0.2}$ and flow properties of materials that obey the Johnson-Cook constitutive model from spherical indentation tests.

Wang et al. [10] used the indentation technique to obtain the properties of the Inc718 at high temperatures. They compared the regularly produced parts and the parts with the modified percentage of ingredients.

Beirau et al. [11] used nanoindentation high-resolution mapping to probe the mechanical properties, indentation hardness (H), and elastic modulus (E) of a natural, highly zoned zircon ($ZrSiO_4$). The results also illustrate how multilayered ceramics accommodate volume expansion and change in mechanical properties as a function of radiation dose.

Bor et al. [12] investigated the elastic modulus, hardness, and fracture toughness of bulk poly-super crystalline nanocomposites of oleic acid-functionalized iron oxide nanoparticles. The underlying micromechanical deformation mechanisms were analyzed for the first time, for materials with and without organic crosslinking ligands by nanoindentation.

Lu et al. [13] employed neural networks and the IIT technique to derive the elastoplastic properties of alloys with acceptable accuracy. They suggested desired algorithms for solving inverse problems using single, dual, and multiple indentations.

In addition to the published research regarding the determination of properties and mechanical behavior of materials using the IIT method, other research has been developed to investigate the causes of errors and improve the accuracy of computations.

Kese et al. [14] studied the properties of soda-lime glass

and found that stress significantly impacts mechanical properties. Also, the results have been improved considering the piling-up phenomenon around the indentation point. Zhao et al. [15] proposed an enhanced technique to determine elastic modulus and yield stress of a linear elastic - perfectly plastic residual stressed bulk material. They expressed that the uniaxial residual compression requires a higher force to indent the material whereas uniaxial residual tension requires a lower force. Huang et al. [16] employed nano-scratch and nanoindentation techniques to assess the influence of residual stress on mechanical properties in thin films. They concluded that modulus and stiffness have decreased by reducing compression and increasing tensile stresses. Khan et al. [17] investigated the effect of residual stresses on the nanoindentation response of aluminum alloys in aerospace. They applied experimental and finite element methods for analyzing the process. They found that residual stresses significantly impacted the maximum force, the curvature of the force-displacement curve, and the achieved properties.

Yetna et al. [18] studied mechanical tensile properties by spherical macro-indentation using an indentation strain-hardening exponent. They found that to improve the indentation-tensile relationship, an additional correction related to the piling-up or sinking-in formation around the indent must be taken into account for the calculation of the strain by indentation. The correction factor is expressed as a function of the strain-hardening exponent.

Li et al. [19] reviewed several existing analytical methods, such as the representative stress-strain method, dimensional analysis method, and inverse finite element method. They first gave an overview of these analytical methods, their advantages, and disadvantages, and introduced ideas to improve them. Skordaris et al. [20] conducted a study on Physical Vapor Deposition (PVD) films and concluded that residual stresses have a considerable influence on determining the properties of films. Scales et al. [21] evaluated over 80 segments of line pipe through tensile testing, IIT, and compositional testing by Optical Emission Spectroscopy (OES) and laboratory combustion. IIT measurements of Ultimate Tensile Stress (UTS) were, generally, in better agreement with destructive tensile data than YS and exhibited about half as much variability as YS measurements on the same sample.

As represented above, there are few studies about the influence of residual stresses on the technique's accuracy in determining the properties and estimating the stress-strain curve. So, it is essential to develop some studies on using the indentation technique in the presence of residual stresses. Also, it is necessary to assess its errors and correct the results.

Because of the wide usage of austenitic steels in industries and the importance of accurate estimating of mechanical properties on manufactured parts, for developing IIT, this research was planned and done. In this study, numerical analysis and experimental tests have been used to evaluate the error of estimating mechanical properties and obtaining stress-strain curves on austenitic steels specimen with equibiaxial residual stresses by IIT. Some $P-h$ analysis

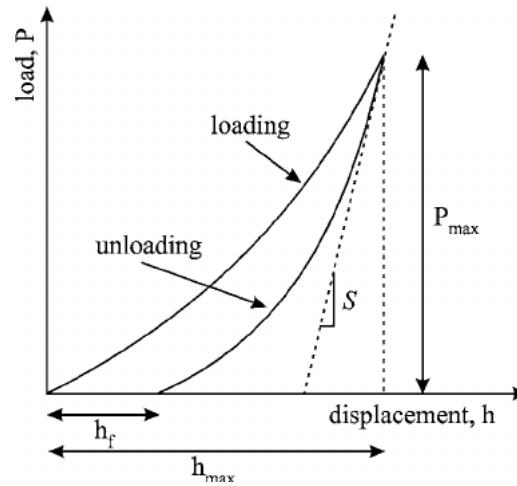


Fig. 1. Indentation load-depth curve for the loading and unloading phases [19]

methods were considered and the method with the relative least errors was selected and then the impact of the stress field was quantitatively assessed. As a novelty of this research, a method was proposed to improve the IIT technique for the accurate estimation of mechanical properties in austenitic steels.

2- Theoretical Background

The analysis of the load-depth curve enables the analyst to obtain elastic modulus, work hardening, yield stress, and in general the mandatory parameters for drawing the stress-strain curve. Fig. 1 shows the data obtained from a typical indentation test. In this figure, P is the applied force, and h is the depth of penetration of the indenter from the primary surface. Three significant parameters are derived from the $P-h$ curve, including maximum force (P_{max}), maximum indenting depth (h_{max}), and elastic unloading stiffness ($S = dP / dh$), which is the slope of the curve at the beginning of the unloading phase.

According to the ASTM E2546-15, the value of S is determined by adapting the unloading curve to the following equation [22]:

$$P = m(h - h_f)^n \quad (1)$$

where m and n are the constants for the power-law, and h_f is the ultimate indenting depth.

To investigate the stress and strain distribution in the indentation area in materials with elastic-plastic deformation, it is necessary to provide the parameters of contact depth (h_c) and contact area of the indenter (A_c) (determined by evaluating the indentation geometry). There is a difference between the contact depth and the measured indentation

depth. This issue is due to the plastic deformation in the contact area. The contact depth (h_c) and contact area (A_c) are computed as follows [23]:

$$h_c = h_{max} - 0.75 \frac{P_{max}}{S} \quad (2)$$

$$A_c = \pi(2Rh_c - h_c^2) \quad (3)$$

The effective elastic modulus (E_{eff}) is defined by the following equation. It is defined based on the fact that the elastic deformation occurs both in a sample with elastic modulus E and Poisson's ratio ν and an indenter with elastic modulus E_i and Poisson's ratio of ν_i [23].

$$\frac{1}{E_{eff}} = \frac{1 - \nu^2}{E} + \frac{1 - \nu_i^2}{E_i} \quad (4)$$

The effective elastic modulus is attained by its relationship to the contact area and the slope of the unloading curve in maximum load as follows [23]:

$$E_{eff} = \frac{S}{2} \frac{\sqrt{\pi}}{\sqrt{A_c}} \quad (5)$$

Since the indenters are often made of tungsten carbide, $\nu_i = 0.07$ and $E_i = 1170$ GPa have been used for experimental tests, and $E_i = \infty$ has been considered for a

perfectly rigid indenter in simulations. Also, the actual elastic modulus has been gained by Eq. (4) [24].

There are different methods for determining the material properties and drawing a stress-strain curve, consisting of Representative stress and strain [25] or Kim method [26], Inverse analysis by FEA [25], Neural networks [25], and Lee method [3]. The Inverse analysis by FEA needs special software, and the Neural networks take more testing time by multiple creep processes. Therefore, these methods are practically difficult and time-consuming. Consequently, the first and fourth methods have been selected for further investigation in this paper.

In the Representative stress and strain or Kim method, the true stress-strain points on the tensile curve are derived by computing the stress and strain in different material depths. This procedure is implemented using a spherical indenter and experimental formulas. Assuming an initial value for n and placing this value in a second-order experimental equation in terms of n and h_{\max}/R , makes it possible to compute the actual contact depth (h_c) and the actual contact area (A_c). The true strain is defined by the $\tan \theta$ (contact angle gradient), and the true stress is defined by the F_{\max} obtained from the load-depth curve and the actual contact area (A_c). The true stress-strain points coincide with an equation such as $\sigma_r = K \varepsilon_r^n$ for the materials with work hardening exponent. If the new n matches with the assumed n , the calculation is terminated, and the obtained values are correct. Otherwise, the average value of the calculated and assumed n is new n , and the calculation is repeated. In all methods, the stress-strain curve has been drawn up to the ultimate strength point. In this case, the areas after this point until the occurrence of rupture are the damaged areas. The advantages of this method are its computational algorithm, applying the information of different depths, and obtaining average results. The disadvantages of this method are concerned with its rigid algorithm and numerical estimations of empirical parameters.

Lee et al. [3] utilized a finite element method and found that the material properties are a function of two factors, including the work hardening coefficient and yield strain. To begin the calculations, it is necessary to formulate the $c^2 (= h_c/h_{\max})$, equivalent plastic strain (ε_p), and plastic constraint factor (ψ) as a function of work hardening coefficient (n), and relative depth (h_{\max}/D). In this case, D is the indenter diameter. The regression coefficients are derived using the finite element method and considering the constant yield strain (ε_0) and 13 different values for n . Then, other regression coefficients can be derived by fixing the value of n and considering three different values for ε_0 . New coefficients are achieved by combining the obtained coefficients. These are the regression constants, which are specified in the appendix of Lee et al. [3] The computational procedure is comprised of performing an indentation test and deriving the force P , depth h , and initial unloading slope S . Then, the initial estimation is carried out for the work hardening coefficient (n) and yield strain (ε_0). Afterward,

the equivalent plastic strain (ε_p), true stress (σ_r) and total strain (ε_t) are computed by the sum of the estimated yield strain (ε_0) and equivalent plastic strain (ε_p). Thereafter, the power curve is fitted to $\sigma_r = K \varepsilon_r^n$. In this case, the stress and strain are known, and the regression analysis derives the K , and new n . Thus, the new elastic modulus, stress, and yield strain are calculated. Also, the relative errors between the new and assumed n and ε_0 are ascertained. If the error in both cases is less than a specific tolerance, the procedure is terminated. Otherwise, the initial assumptions are changed, and the solving procedure is repeated. The principal benefit of this approach refers to its low number of indentations. The disadvantage of this approach refers to its complexity, its numerous steps, and using many coefficients that must be available.

3- Numerical Analysis and Simulations

Since the loading conditions are symmetric, the two-dimensional simulations with an equibiaxial residual stress field seem to be an appropriate way to determine the accuracy of the mentioned two methods in austenitic steels. On the other hand, since the Kim and Lee methods are compared under the same conditions, it is assumed that the superiority of each in two-dimensional simulation can also be generalized to three-dimensional conditions. Also, two-dimensional simulation is cost-effective due to the number of simulations and their time. It seems to be sufficient to obtain the error function, greatly improves the results, and in general, the use of this type of simulation serves our purpose.

The simulated model deals with two parts: consisting of a rigid indenter part and a flexible bottom part. To create a geometric symmetry, the indenter part is in the form of a quarter circle with a diameter of 1.58 mm (1/16 in), and the part under test (it is half of the bottom object) is a square with the dimensions of 10 mm \times 10 mm. Its elements are in the form of a symmetric eight-node of CAX8R with the number 10000. Fig. 2 shows how it converges in 10000 elements. The smallest size of elements beneath the indenter is approximately 1 μ .

The tensile and compressive residual stresses are applied through pressure on the edge of the bottom part. Fig. 3 shows the boundary conditions for the two-dimensional model. In the bottom part, the finer meshes have been considered for the regions around the contact area. It was due to the severe local deformation under the indenter. To validate the accuracy of the modeling and the specified interval of properties, a piece of stainless steel has been subjected to a standard tensile test based on the ASTM E8/E8m 13a. In this case, the elastic modulus has been gained based on ASTM E111-97, and the yield stress and work hardening coefficient have been captured through fitting to a power curve. The results of these computations are given in Table 1.

The part is assumed as a von Mises elastoplastic material with isotropic hardening behavior. The stress-strain relationship in the sample is defined as Eq. (6) [27].

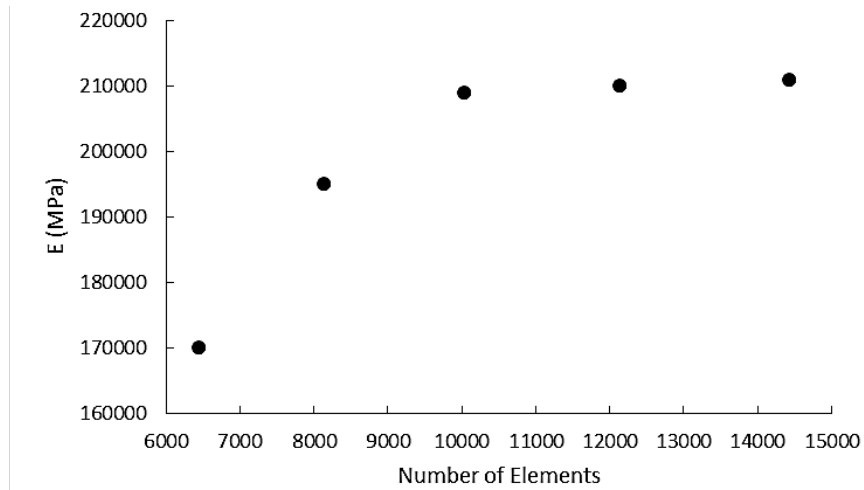


Fig. 2. Results convergence with different elements in mesh effect study

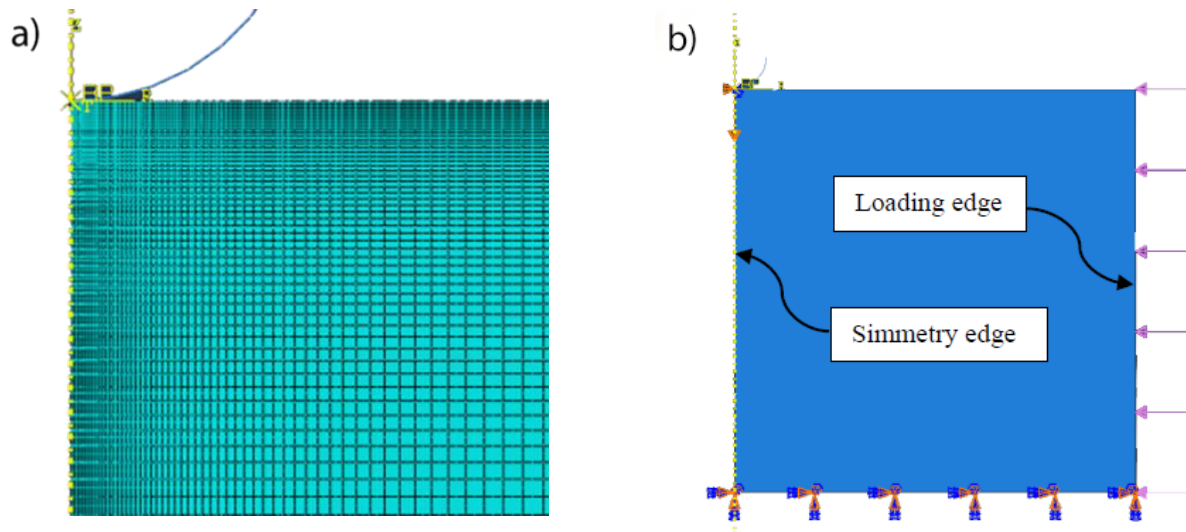


Fig. 3. The finite element model: (a) indentation area and mesh density, (b) two-dimensional boundary conditions.

Table 1. The obtained properties of sample steel (SS321) via the tensile test.

Material	Young's modulus E (MPa)	Yield strength σ_y (MPa)	Work hardening exponent n
SS321	204000 (± 9823)	306 (± 7.8)	0.14 (± 0.0058)

Table 2. The range of properties of the studied materials and their loading conditions in the simulation.

Young's modulus, E	200 GPa				
Yield stress, σ_y	300 MPa				
Work hardening exponent, n	0.1	0.15	0.2		
Ratio of residual stress to yield stress, σ_r / σ_y	0	± 0.3	± 0.5	± 0.7	± 0.9

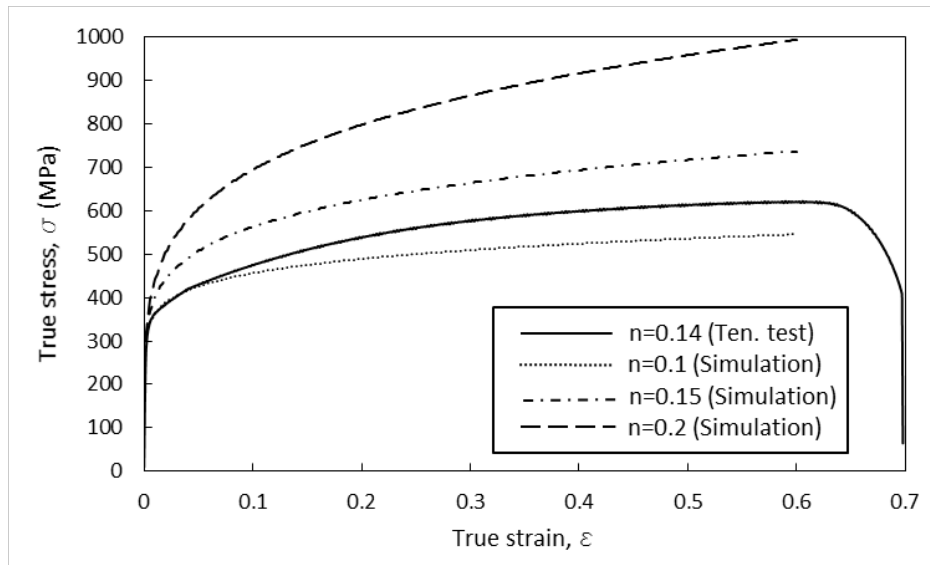


Fig. 4. Stress-strain curve of austenitic steel obtained from the standard tensile test and true stress-true strain curves of the material were taken into account for simulations

$$\sigma = \begin{cases} E \varepsilon & \varepsilon \leq \sigma_y / E \\ R \varepsilon^n & \varepsilon \geq \sigma_y / E \end{cases} \quad (6)$$

where $R = \sigma_y (E / \sigma_y)^n$.

In this study, the elastic modulus and yield strength were considered 200 GPa and 300 MPa, respectively. It was due to their small changes in austenitic steels. The properties of materials and loading conditions are provided in Table 2.

A total number of 27 two-dimensional simulations have been implemented to evaluate all feasible scenarios. According to the work hardening coefficient derived from the tensile test, three different work hardening coefficients ($n = 0.1, 0.15, \text{ and } 0.2$) were considered to cover the behavioral range of austenitic steels. Fig. 4 depicts the stress-strain curve

for the sample of austenitic stainless steel and the stress-strain curve for the simulated materials with different powers n according to Eq. (6).

Fig. 5 depicts the typical results of the simulations as a load-depth curve for steel with $n = 0.14$ in different residual stresses. Also, their deviations from the stress-free state are indicated in this figure. As illustrated, the tensile and compressive residual stresses push them lower and upper than the free-stress curve, respectively.

To validate the results of the finite element simulations, a cross-shaped specimen made of SS321 is considered in this study. The first step is to relieve stress from the specimen. According to AZO Materials [28], the specimen is placed in a furnace at a temperature of 700 °C for 90 minutes. Then, it is cooled at ambient temperature and placed in a loading fixture according to Moharrami and Sanayei [29]. The strain

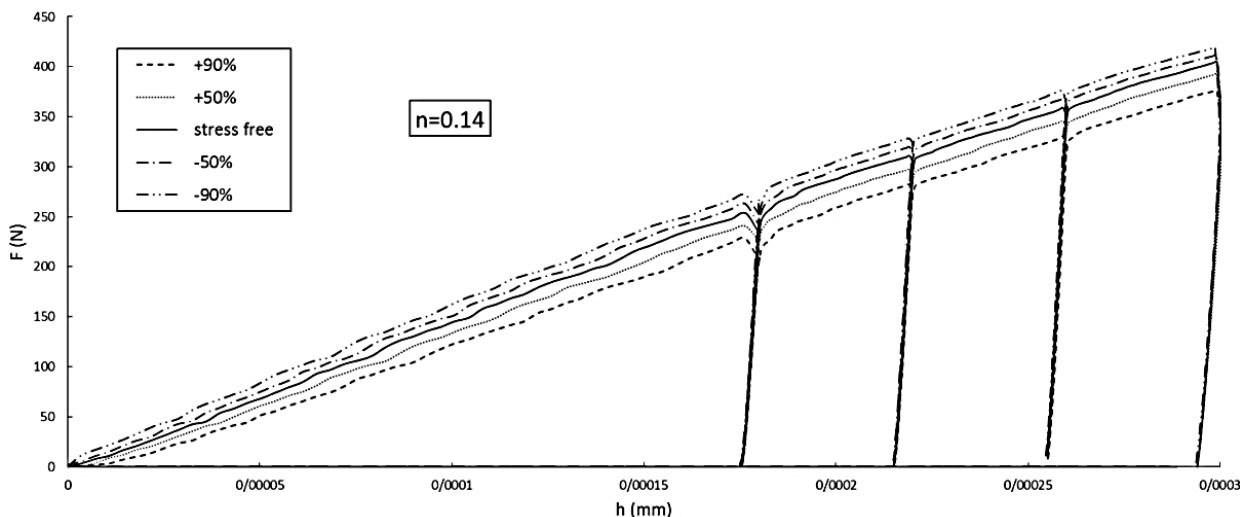


Fig. 5. The load-depth curves for the steel indentation test with $n = 0.14$ in various normalized residual stresses (σ_r/σ_y) .

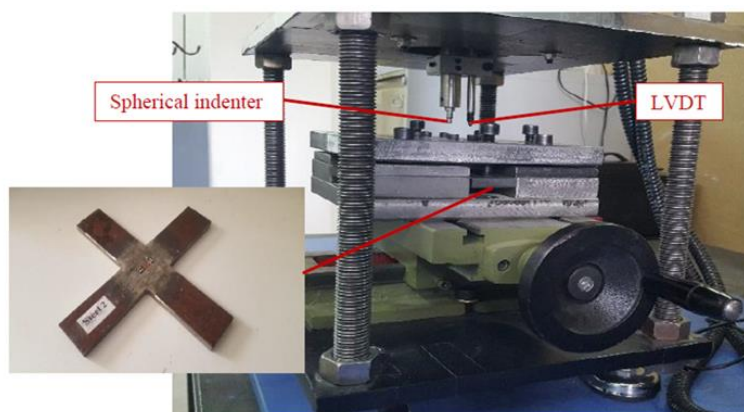


Fig. 6. Test setup including a cross-shaped specimen with the strain gauge mounted on it, a bending fixture, and indentation apparatus.

is applied by straining screws, and a perpendicular gauge rosette captures its value. After that, an indenter of 1.58 mm (1/16 in) performs the indentation test. To provide the quasi-static conditions, the indentation tests were implemented at a loading rate of 0.2 mm/min and a straining rate of 0.08 s⁻¹ [30]. Fig. 6 indicates several details, including the cross-shaped specimen with magnifying the strain gauge rosette, and the test set.

4- Analysis of Results

In this study, the accuracy of the two methods was

investigated by comparing the calculated properties and the properties applied to the finite element model in austenitic stainless steel. In each case, the error of computation is formulated for the property of I as follows [31]:

$$error = \frac{I_{cal} - I_{app}}{I_{app}} \times 100 \quad (7)$$

where I_{app} characterizes the value of the applied

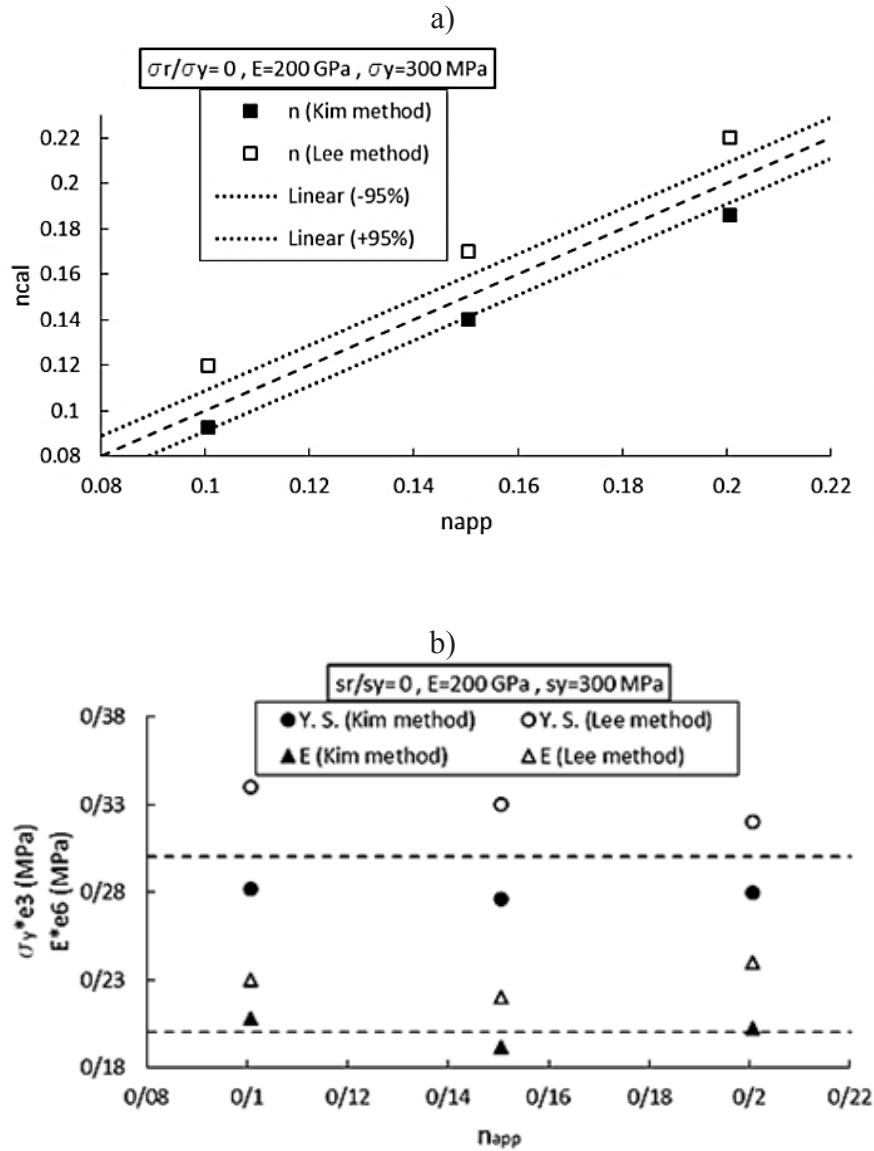


Fig. 7. A comparison of the calculated properties with the applied work hardening at different residual stresses a) Work hardening and b) Elastic modulus and Yield stress.

property to the model, and I_{cal} expresses the value of the calculated property via the assumed method. Fig. 7 provides the graphical representation of the error in the mechanical property calculated via the mentioned methods.

As shown in this figure, in the absence of residual stresses, the applied work hardening coefficients are shown on the horizontal axis, and the computed work hardening coefficient, yield stress, and elastic modulus are shown on the vertical axis. In figure (a), the dashed line denotes the ideal situation where the computed work hardening coefficient is equal to its applied value. It is observed that the results of Kim's method are closer to the ideal line. The average relative error of the Lee method is 15% and that of the Kim method is 7%.

In figure (b), the achieved values for the yield stress and elastic modulus are compared to the applied constant values

of 300 MPa and 200 GPa, respectively. These comparisons are displayed through a dashed line. The comparison between the two methods demonstrated that the Kim method was closer to the given value. In this method, the results of n are more accurate in small values, while no specific pattern is observed for E and σ_y . The results of the computed property error in the equibiaxial residual stresses showed that the Kim method provided more accurate simulation results than the Lee method. Therefore, the Kim method has been considered to obtain the properties of materials and plot the stress-strain curve. Fig. 8 indicates the stress-strain curve plotted by the Kim method for the residual stresses, which correspond to the stresses expressed in Fig. 5. Also, their deviations from the stress-free state are denoted in this figure. It was observed that an increase in the residual stress

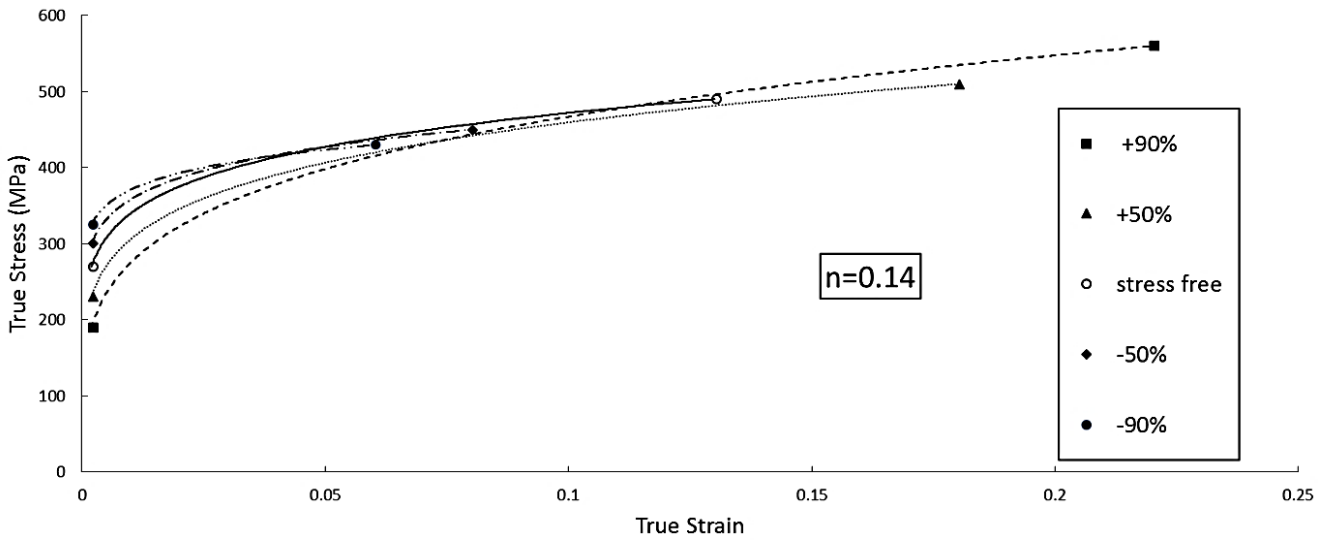


Fig. 8. The plastic region for the steel stress-strain curves with $n = 0.14$ in the variation of normalized residual stresses (σ_r/σ_y) (plotted by the Kim method).

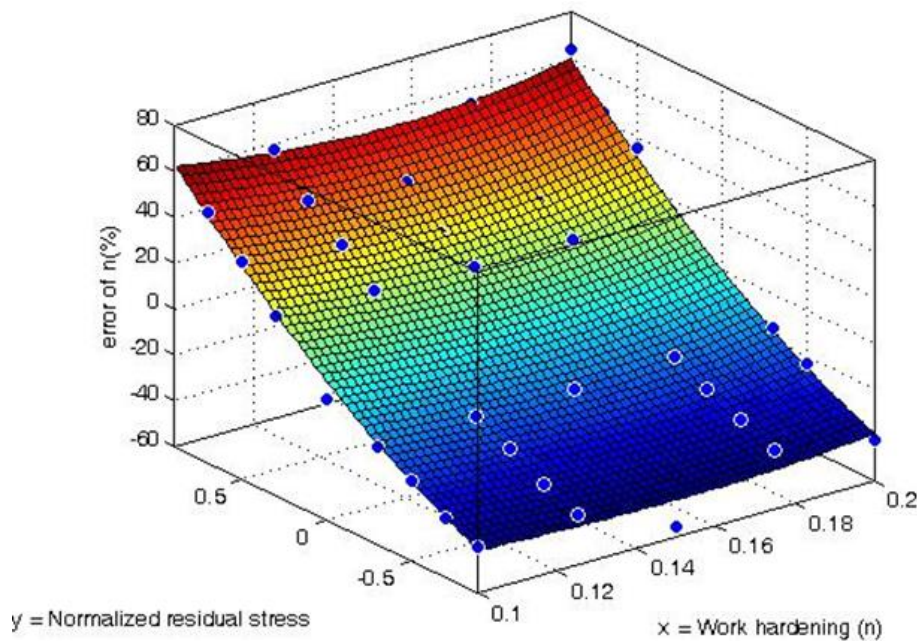


Fig. 9. The error of work hardening measurement by the Kim method.

raised the computation error. Thus, the values of properties deviate from their correct values. Indeed, the elastic modulus and yield stress have gradually decreased by moving from the compressive stresses to the tensile stresses. In contrast, the work-hardening values have gradually increased. The result obtained also agrees with [32]. They have stated that in materials with similar hardness, a material with a relatively low modulus of elasticity has a high work hardening and a material with a relatively high modulus of elasticity has a low work hardening.

Fig. 9 demonstrates the graphical results for computing the error of the work hardening value. In all cases, a third-order equation of a plane is fitted to the raw data.

Likewise, the surface can be drawn for the yield stress and elastic modulus. Figs. 10 and 11, illustrate the errors as a third-order function of the work hardening and normalized residual stress (σ_r/σ_y) . The maximum error and rate of error changes in tensile and compressive stresses are not the same on these surfaces. If an increase occurs in the tensile residual stresses, the rate of changes in the error of properties

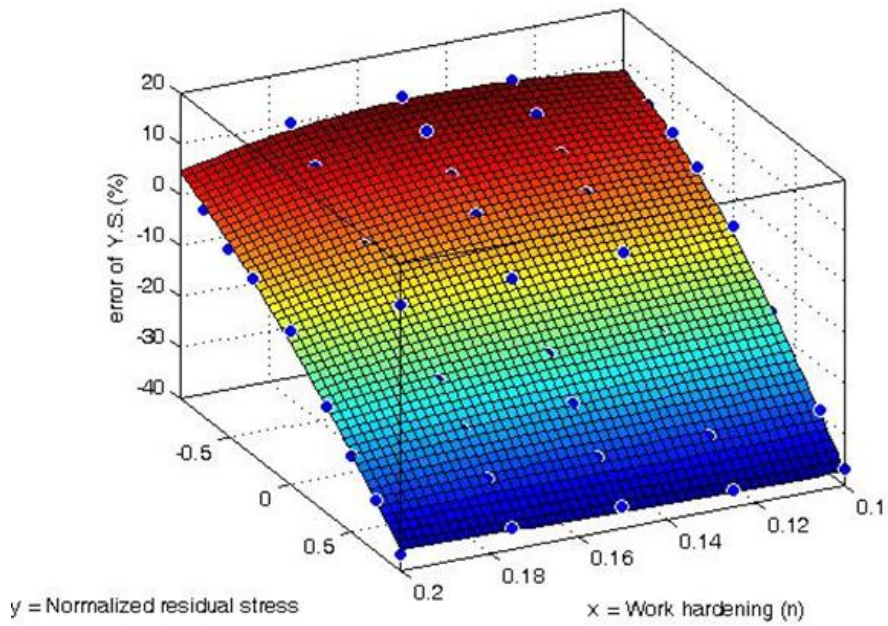


Fig. 10. The error of yield stress measurement by the Kim method.

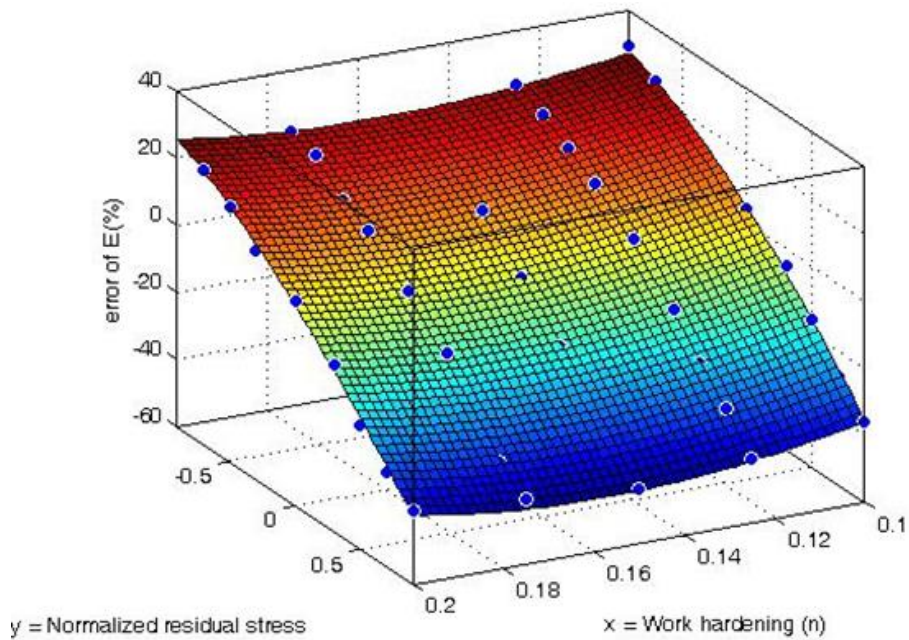


Fig. 11. The error of elastic modulus measurement by the Kim method.

in tensile residual stresses becomes greater than its rate in compressive residual stresses. This issue leads to a change in the slope of the surface created around the zero-stress regions. Also, the maximum error in the tensile zone is greater than that in the compressive zone, and up to a 100% increase in errors is observed.

The significant effect of stress on the results of estimating mechanical properties using this technique, which has been obtained in this study, has been confirmed in reports

published by other researchers. Although no similar work has been reported on the subject of research presented in this article, but some results from the study on the effect of residual stresses on the estimation of some mechanical properties are shown in Fig. 12 a [14] and b [16]. These show the trend of deviation in estimated elasticity modulus and hardness number versus residual stresses. In this study, for quantitative analysis, based on Figs. 9 to 11 the general form of error variation was assumed with a function of n , σ_r/σ_y ,

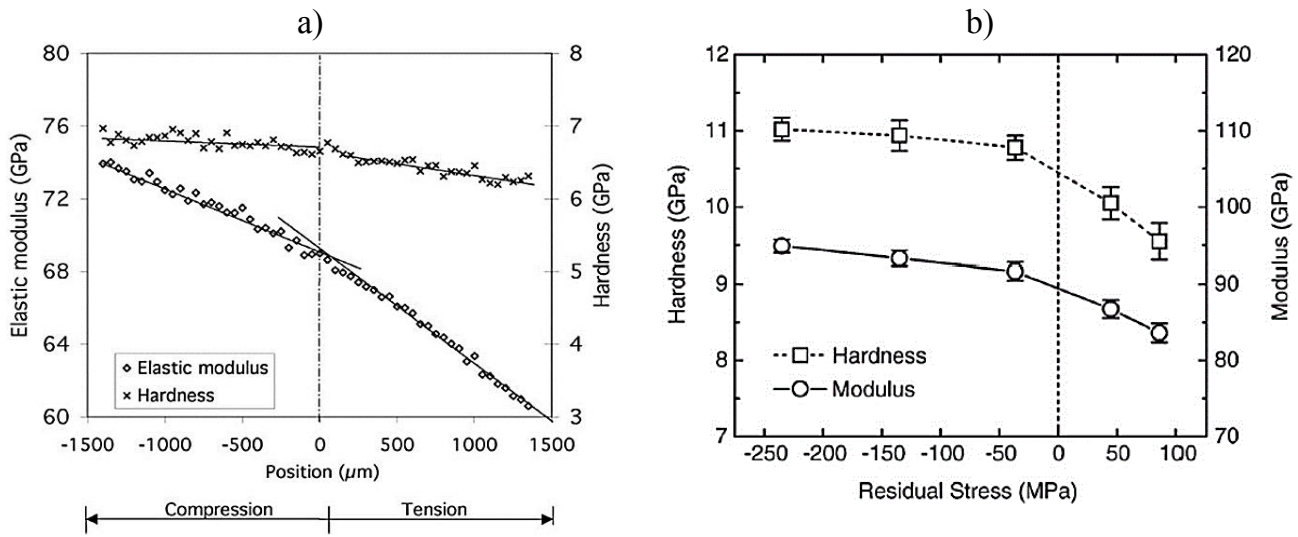


Fig. 12. The effect of residual stresses on elasticity modulus and the slope of its changes a) [14], b) [16].

Table 3. The modified values of arbitrary properties via the proposed method in this paper.

Applied stress and property		Calculated property by Kim method			Error (%)			Corrected property by the suggested method			Error after correction (%)		
σ_r/σ_y	n	n	σ_y (MPa)	E (GPa)	n	σ_y	E	n	σ_y (MPa)	E (GPa)	n	σ_y	E
-0.21	0.11	0.1	295	218	-10	-2	9	0.11	303	212	0	1	6
0.55	0.14	0.19	230	145	36	-23	-28	0.15	305	185	7	2	-8
-0.85	0.17	0.1	324	244	-41	8	22	0.16	299	191	-6	0	-5

and it is expressed as follows:

$$f(x, y) = ax + bx^2 + cx^3 + a'y + b'y^2 + c'y^3 + a''xy + b''x^2y + c''xy^2 + d \quad (8)$$

where $x = n$ is the work hardening coefficient and $y = \sigma_r/\sigma_y$ is the normalized residual stress.

If the error changes for the stresses and various work hardenings are considered, the error functions can be formulated as unique functions of $f(n, \sigma_r/\sigma_y)$. Thus, it is possible to determine the difference between the computed property value and its applied value. Using the procedure proposed in this study and Eq. (9), the properties of austenitic

stainless steels can be recalculated as follows:

$$I_{corrected} = \frac{I_{calculated}}{1 + f(n, \sigma_r/\sigma_y)} \quad (9)$$

Table 3 gives some examples of the modified values of properties via the proposed method in this paper.

The computed properties experimentally for the SS321 alloy (Fig. 6) in different residual stresses have been modified by the method proposed in this paper. The results of the computations are given in Table 4. As an example, the first row of the table is plotted in Fig. 13. In this figure, the curve obtained from the tensile test without the residual stress is

Table 4. The results of applying the proposed method for modifying the experimental properties of SS321.

Applied stress and property		Calculated property by Kim method			Error (%)			Corrected property by the suggested method			Error after correction (%)		
σ_r/σ_y	n	n	σ_y (MPa)	E (GPa)	n	σ_y	E	n	σ_y (MPa)	E (GPa)	n	σ_y	E
0.8	0.14	0.203	201	123	45	-33	-39	0.139	302	195	-1	1	-3
-0.8	0.14	0.073	324	239	-48	8	20	0.156	298	183	12	-1	-9
-0.6	0.14	0.075	313	230	-46	4	15	0.127	296	187	-10	-1	-7

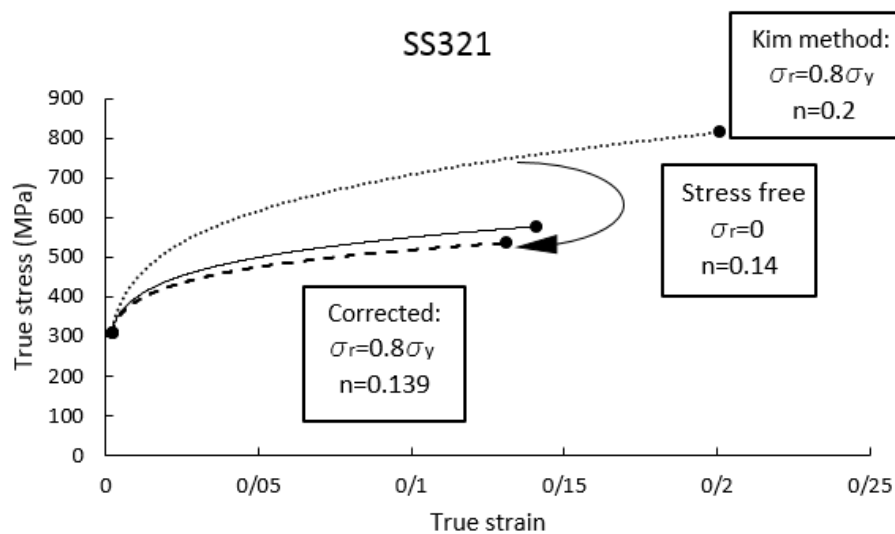


Fig. 13. The indentation stress-strain curve before and after modification.

compared to the curve derived from the Kim method by the indentation test in the presence of residual stresses. Also, it is compared to its modified curve.

5- Conclusions

In this paper, the indentation method has been employed to investigate the Kim and Lee methods for calculating the properties of materials in the equibiaxial residual stress field. Since the loading process and residual stresses are symmetric, two-dimensional finite element simulation has been utilized in this study. Experimental tests were performed to validate the simulation results. The research results are described one by one below:

The Lee method deals with an average error of 15% for the calculation of the properties under stress-free conditions while the Kim method has a maximum error of 7% in the same condition. Consequently, the Kim method has been selected for further investigations.

In the Kim method, the results of n are more accurate in

small values.

The elastic modulus and yield stress have gradually decreased by moving from the compressive stresses to the tensile stresses. In contrast, the work-hardening values have gradually increased.

In the Kim method, the rate of error changes for computing the material properties in the compressive stress field is less than in the tensile stress field. The maximum error in the tensile zone is greater than that in the compressive zone, and up to a 100% increase in errors is observed, which can be due to cavities and cracks that are sensitive to tensile stress.

By evaluating and formulating the error changes in the achieved results as a function of work hardening n and normalized residual stress σ_r/σ_y , a method has been proposed to predict and eliminate the Kim method's error.

The proposed method has significantly mitigated the error in computing the properties of materials with residual stresses through the Kim method as follows:

In the numerical analysis study, the absolute value of

errors has decreased from a maximum 41% for n , 23% for σ_y , and 28% for E to 6%, 2%, and 8%, respectively.

In the experimental test, the results look better, and the absolute value of errors has decreased from a maximum of 48% for n , 33% for σ_y , and 39% for E to 12%, 1%, and 3%, respectively.

References

- [1] D. Tabor, A simple theory of static and dynamic hardness, *Proceedings of the Royal Society of London. Series A. Mathematical and Physical Sciences*, 192(1029) (1948) 247-274.
- [2] M.F. Doerner, W.D. Nix, A method for interpreting the data from depth-sensing indentation instruments, *Journal of Materials research*, 1(4) (1986) 601-609.
- [3] H. Lee, J.H. Lee, G.M. Pharr, A numerical approach to spherical indentation techniques for material property evaluation, *Journal of the Mechanics and Physics of Solids*, 53(9) (2005) 2037-2069.
- [4] S.H. Kim, B.W. Lee, Y. Choi, D. Kwon, Quantitative determination of contact depth during spherical indentation of metallic materials—A FEM study, *Materials Science and Engineering: A*, 415(1-2) (2006) 59-65.
- [5] J.H. Lee, T. Kim, H. Lee, A study on robust indentation techniques to evaluate elastic-plastic properties of metals, *International Journal of Solids and Structures*, 47(5) (2010) 647-664.
- [6] A. Boschetto, F. Quadri, E.A. Squeo, Extracting local mechanical properties of steel bars by means of instrumented flat indentation, *Measurement*, 44(1) (2011) 129-138.
- [7] Z. Chunyu, Z. Yulong, C. Youbin, C. Nanfeng, C. Lei, Understanding indentation-induced elastic modulus degradation of ductile metallic materials, *Materials Science and Engineering: A*, 696 (2017) 445-452.
- [8] C. Chang, M. Garrido, J. Ruiz-Hervias, Z. Zhang, L.-l. Zhang, Representative stress-strain curve by spherical indentation on elastic-plastic materials, *Advances in Materials Science and Engineering*, 2018 1-9.
- [9] T. Zhang, S. Wang, W. Wang, Determination of the proof strength and flow properties of materials from spherical indentation tests: an analytical approach based on the expanding cavity model, *The Journal of Strain Analysis for Engineering Design*, 53(4) (2018) 225-241.
- [10] H. Wang, A. Dhiman, H.E. Ostergaard, Y. Zhang, T. Siegmund, J.J. Kruzic, V. Tomar, Nanoindentation based properties of Inconel 718 at elevated temperatures: A comparison of conventional versus additively manufactured samples, *International Journal of Plasticity*, 120 (2019) 380-394.
- [11] T. Beirau, W.C. Oliver, C.E. Reissner, W.D. Nix, H. Pöllmann, R.C. Ewing, Radiation-damage in multi-layered zircon: Mechanical properties, *Applied Physics Letters*, 115(8) (2019) 081902.
- [12] B. Bor, D. Giuntini, B. Domènech, M.V. Swain, G.A. Schneider, Nanoindentation-based study of the mechanical behavior of bulk supercrystalline ceramic-organic nanocomposites, *Journal of the European Ceramic Society*, 39(10) (2019) 3247-3256.
- [13] L. Lu, M. Dao, P. Kumar, U. Ramamurty, G.E. Karniadakis, S. Suresh, Extraction of mechanical properties of materials through deep learning from instrumented indentation, *Proceedings of the National Academy of Sciences*, 117(13) (2020) 7052-7062.
- [14] K. Kese, Z. Li, B. Bergman, Influence of residual stress on elastic modulus and hardness of soda-lime glass measured by nanoindentation, *Journal of materials research*, 19(10) (2004) 3109-3119.
- [15] M. Zhao, X. Chen, J. Yan, A.M. Karlsson, Determination of uniaxial residual stress and mechanical properties by instrumented indentation, *Acta Materialia*, 54(10) (2006) 2823-2832.
- [16] Y.-C. Huang, S.-Y. Chang, C.-H. Chang, Effect of residual stresses on mechanical properties and interface adhesion strength of SiN thin films, *Thin Solid Films*, 517(17) (2009) 4857-4861.
- [17] M. Khan, M. Fitzpatrick, S. Hainsworth, L. Edwards, Effect of residual stress on the nanoindentation response of aerospace aluminium alloys, *Computational Materials Science*, 50(10) (2011) 2967-2976.
- [18] M.Y. N'Jock, D. Chicot, X. Decoopman, J. Lesage, J. Ndjaka, A. Pertuz, Mechanical tensile properties by spherical macroindentation using an indentation strain-hardening exponent, *International Journal of Mechanical Sciences*, 75 (2013) 257-264.
- [19] Y. Li, P. Stevens, M. Sun, C. Zhang, W. Wang, Improvement of predicting mechanical properties from spherical indentation test, *International Journal of Mechanical Sciences*, 117 (2016) 182-196.
- [20] G. Skordaris, K. Bouzakis, T. Kotsanis, P. Charalampous, E. Bouzakis, B. Breidenstein, B. Bergmann, B. Denkena, Effect of PVD film's residual stresses on their mechanical properties, brittleness, adhesion and cutting performance of coated tools, *CIRP Journal of Manufacturing Science and Technology*, 18 (2017) 145-151.
- [21] M. Scales, J. Anderson, J.A. Kornuta, N. Switzer, R. Gonzalez, P. Veloo, Accurate Estimation of Yield Strength and Ultimate Tensile Strength through Instrumented Indentation Testing and Chemical Composition Testing, *Materials*, 15(3) (2022) 832.
- [22] ASTM, Standard practice for instrumented indentation testing, in, *ASTM E2546-15*, 2015.
- [23] A.C. Fischer-Cripps, in: *Nanoindentation*, Springer New York, 2011, pp. 21-37.
- [24] A. Fischer-Cripps, Elastic recovery and reloading of hardness impressions with a conical indenter, *MRS Online Proceedings Library (OPL)*, 750 (2002).
- [25] Iso, *Metallic materials - Measurement of mechanical*

- properties by an instrumented indentation test - Indentation tensile properties, in, ISO/TR 29381, 2008.
- [26] J.-Y. Kim, K.-W. Lee, J.-S. Lee, D. Kwon, Determination of tensile properties by instrumented indentation technique: Representative stress and strain approach, *Surface and Coatings Technology*, 201(7) (2006) 4278-4283.
- [27] J. Yan, A.M. Karlsson, X. Chen, Determining plastic properties of a material with residual stress by using conical indentation, *International journal of solids and structures*, 44(11-12) (2007) 3720-3737.
- [28] AZOMaterials, Stainless Steel - Grade 321 (UNS S32100), in: <https://www.azom.com/article.aspx?ArticleID=967>., 2001.
- [29] R. Moharrami, M. Sanayei, Developing a method in measuring residual stress on steel alloys by instrumented indentation technique, *Measurement*, 158 (2020) 107718.
- [30] R. Misra, Z. Zhang, Z. Jia, P.V. Surya, M. Somani, L. Karjalainen, Nanomechanical insights into the deformation behavior of austenitic alloys with different stacking fault energies and austenitic stability, *Materials Science and Engineering: A*, 528(22-23) (2011) 6958-6963.
- [31] M.-J. Choi, S.-K. Kang, I. Kang, D. Kwon, Evaluation of nonequibiaxial residual stress using Knoop indenter, *Journal of Materials Research*, 27(1) (2012) 121-125.
- [32] H. Lan, T. Venkatesh, On the relationships between hardness and the elastic and plastic properties of isotropic power-law hardening materials, *Philosophical Magazine*, 94(1) (2014) 35-55.

HOW TO CITE THIS ARTICLE

F. Barati, R. Moharrami, Accurate Estimating of Mechanical Properties of Austenitic Stainless Steels with Residual Stresses Using Indentation Technique, AUT J. Mech Eng., 6(4) (2022) 511-524.

DOI: [10.22060/ajme.2022.20715.6016](https://doi.org/10.22060/ajme.2022.20715.6016)

